



OPEN ACCESS

EDITED BY

Sabrina Arcaro,
University of the Extreme South of Santa
Catarina, Brazil

REVIEWED BY

Ahmed El-Fiqi,
National Research Centre, Egypt
Luis César R. Aliaga,
Rio de Janeiro State University, Brazil

*CORRESPONDENCE

Tian Li,
✉ tian3.li@connect.polyu.hk
Guangping Zheng,
✉ mmzheng@polyu.edu.hk

RECEIVED 14 December 2023

ACCEPTED 01 February 2024

PUBLISHED 16 February 2024

CITATION

Li T, Li N, Kuang B and Zheng G (2024),
Molecular dynamics simulation on the
mechanical properties of Zr-Cu metallic
nanoglasses with heterogeneous chemical
compositions.

Front. Mater. 11:1355522.

doi: 10.3389/fmats.2024.1355522

COPYRIGHT

© 2024 Li, Li, Kuang and Zheng. This is an
open-access article distributed under the
terms of the [Creative Commons Attribution
License \(CC BY\)](https://creativecommons.org/licenses/by/4.0/). The use, distribution or
reproduction in other forums is permitted,
provided the original author(s) and the
copyright owner(s) are credited and that the
original publication in this journal is cited, in
accordance with accepted academic practice.
No use, distribution or reproduction is
permitted which does not comply with
these terms.

Molecular dynamics simulation on the mechanical properties of Zr-Cu metallic nanoglasses with heterogeneous chemical compositions

Tian Li^{1,2,3*}, Nana Li^{1,4}, Bo Kuang¹ and Guangping Zheng^{3*}

¹CDGM Glass Co., Ltd., Chengdu, China, ²Chengdu Guangming Paite Precious Metal Co., Ltd., Chengdu, China, ³Department of Mechanical Engineering, The Hong Kong Polytechnic University, Kowloon, Hong Kong SAR, China, ⁴The Hong Kong University of Science and Technology, Kowloon, Hong Kong SAR, China

The mechanical properties of metallic nanoglasses (NGs) strongly depend on the average size of glassy grains (D_{avg}). Nevertheless, current knowledge on the effects of sizes of glassy grains is incomplete for the mechanical properties of NGs. Herein, Zr_xCu_{100-x} ($25 \leq x \leq 75$) nanoglasses containing glassy grains with different chemical compositions, *i.e.*, the heterogeneous NGs (HNGs), are investigated by molecular dynamics simulation, and the relation between ultimate tensile strength (UTS) and D_{avg} is determined. Specifically, the UTS decreases with decreasing D_{avg} in Zr-Cu HNGs when $D_{avg} < 10$ nm, mainly resulting from the increased volume fraction of glass-glass interfaces, while UTS would follow the Hall-Petch like relation for Zr-Cu HNGs when $D_{avg} > 10$ nm, which is closely related to glassy grains with compositions dominated by Zr atoms. This study provides a deep insight into the mechanical property dependence on grain size in the HNGs, which could be a novel strategy in resolving the issue of strength-ductility tradeoff in NGs.

KEYWORDS

metallic nanoglasses, non-crystalline alloys, mechanical properties, molecular dynamics, grain-size effects

1 Introduction

Metallic glasses (MGs) are amorphous alloys prepared through the melt quenching route (Miroshnichenko and Salli, 1959; Klement et al., 1960). Due to the lack of crystalline defects (Inoue, 1995; Inoue et al., 2003), MGs normally have an ultrahigh mechanical strength, which enables them to become an ideal candidate (Ashby and Greer, 2006; Gu et al., 2007) for the structural applications. However, the issues of intrinsic brittleness have restricted the use of MGs. Recently, planar defects, *i.e.*, glass-glass interfaces (GGIs), are introduced into the amorphous alloys (Jing et al., 1989), resulting in a new type of amorphous alloys, *i.e.*, metallic nanoglasses (NGs) (Fang et al., 2012; Wang C. et al., 2016a; Mohri et al., 2018; Pei et al., 2020; Li and Zheng, 2022a). It is (Gleiter, 2013; 2016; Franke et al., 2014; Gleiter et al., 2014) suggested that NGs are composed of glassy grains as separated by GGIs (Chen et al., 2017), analogous to the microstructures of polycrystalline alloys (Baksi et al., 2020; Cheng et al., 2020; Ghafari et al., 2020; Li and Zheng, 2022b). More

importantly, the ductility of NGs could be much improved, namely, through decreasing the sizes of glassy grains (Wang et al., 2015; Wang et al., 2016b X.; Li et al., 2018; Guo et al., 2019; Nandam et al., 2020; Li and Zheng, 2021; Yang et al., 2021). Nonetheless, mechanical strength of NGs with decreasing sizes of glassy grains would reduce significantly, resulting in strength-ductility tradeoff issue for NGs.

For the first time, mechanical properties of amorphous alloys may be controlled in a new way, *i.e.*, by alternating their microstructures (Voigt et al., 2023a; 2023b; Singh et al., 2023; Vasantham et al., 2023), similar to those applied for crystalline materials, as demonstrated in our previous experimental work (Li et al., 2021a) that the grain-size effects play an important role in tuning the mechanical properties of NGs. From atomistic simulations, Adibi *et al.* (Adibi et al., 2014; 2015) have found that the mechanical strength of NGs would decrease monotonously through reducing the size of glassy grains in NGs with a homogenous chemical composition. Furthermore, their results indicated that the influences of sizes of glassy grains on mechanical strength of NGs is closely related with the chemical compositions of glassy grains. Therefore, it is suggested that the grain-size effects on mechanical properties of NGs containing glassy grains with heterogenous compositions (HNGs) are much different from those observed in NGs with a homogenous composition. However, current knowledge is still lacking for the HNGs, posing an issue needs to be further addressed.

To date, inert gas condensation (Averback et al., 1990; Chen et al., 2015; Nandam et al., 2021), magnetron sputtering (Wang et al., 2014; Ketov et al., 2015; Sniadecki et al., 2016; Mohri et al., 2017; Nandam et al., 2017), severe plastic deformation (Wang et al., 2011; Shao et al., 2013) and pulse electrodeposition (Shen et al., 2011; Guo et al., 2017; Li et al., 2021b) have been developed to fabricate NGs. Despite of the manufacturing routes, the preparation of NGs in large dimensions is still challenging and, as a result, there are only a very few studies (Hu et al., 2017; Sharma et al., 2021) that determine the mechanical properties of NGs through mechanical tests, largely attributing to the fabrication barrier of current techniques. Molecular dynamics (MD) simulation is a versatile tool that could overcome the limitation of experimental methods, which allows us to investigate their mechanical properties at atomistic scales. This approach much relies on the availability of interatomic potentials and most simulation studies (Kalcher et al., 2020; Adjaoud and Albe, 2021; Ma et al., 2021; Yuan and Branicio, 2021) focus on Zr-Cu system since there is a lack of reliable interatomic potentials developed for describing amorphous alloys. Thus, in this work, the Zr-Cu HNG models containing glassy grains with different compositions (Zr_xCu_{100-x} , $25 \leq x \leq 75$) have been constructed for MD simulations to address the aforementioned issues of grain-size effects in HNGs. The simulation results show that, for Zr-Cu HNGs, the ultimate tensile strength (UTS) would decrease and increase through reducing the average size (D_{avg}) of glassy grains when $D_{avg} < 10$ nm and $D_{avg} > 10$ nm, respectively, resulting in grain size effects much different from those observed in NGs composed of glassy grains with a same chemical composition (Adibi et al., 2014; 2015). This work demonstrates that developing HNGs could be a novel approach that would resolve the tradeoff issue of strength-ductility in NGs.

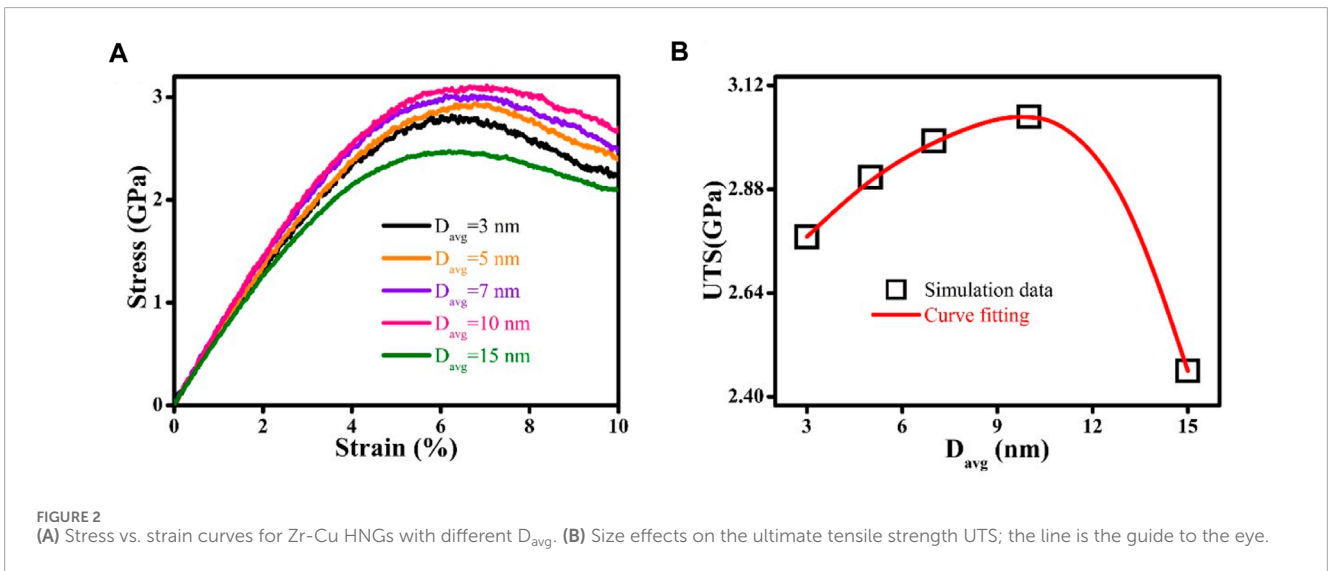
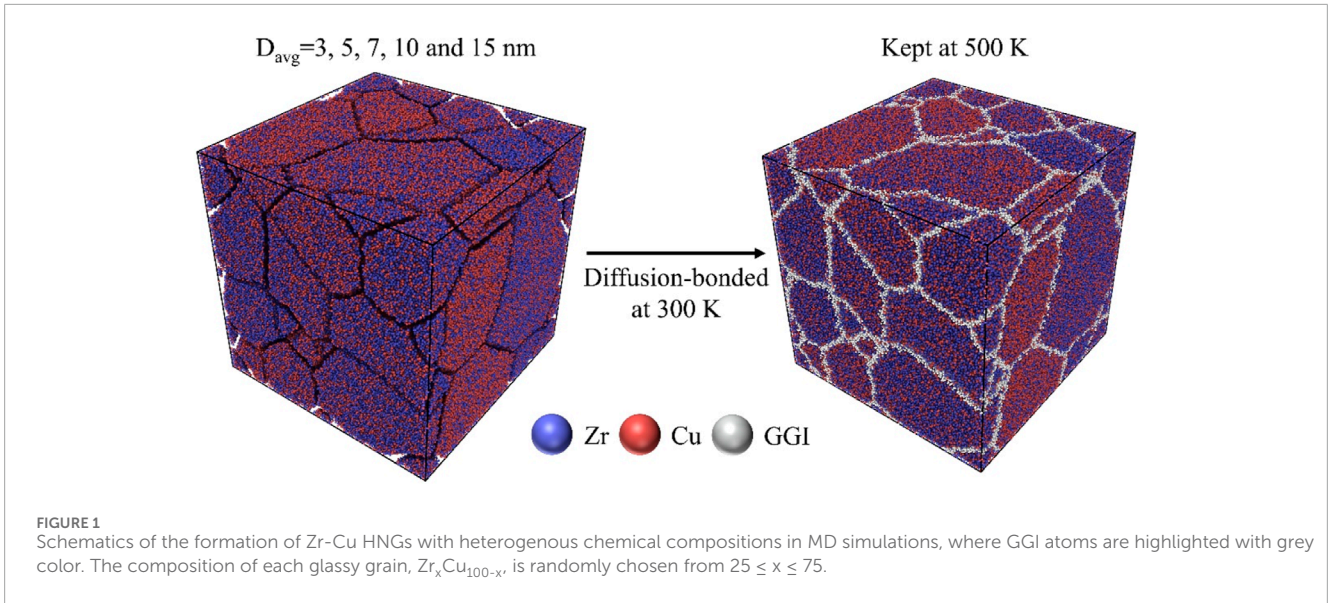
2 Simulation methodologies

MD simulations were performed on the large-scale atomic/molecular massively parallel simulator (Plimpton, 1997). The interatomic potentials between Zr-Zr, Zr-Cu and Cu-Cu were described by the embedded atom method (Mendelev et al., 2009). The potentials have been optimized to simulate the amorphous atomic structures of Zr-Cu glasses accurately, meaning that they can be effective in simulating the mechanical properties of Zr-Cu NGs. The equations of motions were numerically integrated at a timestep of 1 fs, and periodic boundary conditions were applied in x , y and z directions. A barostat and Nose-Hoover thermostat were applied to control the pressure and temperature of simulation cells, respectively.

A crystalline Zr_xCu_{100-x} ($25 \leq x \leq 75$) alloy was initially constructed (Hirel, 2015) and relaxed at 300 K under isobaric-isothermal ensemble. The relaxed crystalline Zr-Cu alloy was first kept at 2,000 K until it was completely transformed into a liquid phase. The melts were then rapidly quenched to 300 K at a cooling rate of 10^{10} K/s, resulting in Zr_xCu_{100-x} ($25 \leq x \leq 75$) MG with a well-defined glass phase. The HNG model systems containing glassy grains with various sizes were constructed by filling Zr_xCu_{100-x} MGs with Zr contents x randomly chosen between 25 and 75 into a nanostructured model system, whose grain sizes and shapes, interfaces and triple junctions among grains could be well tuned to represent those observed in experiments (Zheng et al., 2005). The procedures of construction of HNG model systems were described as follows: First, the Zr_xCu_{100-x} ($25 \leq x \leq 75$) MG models constructed by the MD simulations as described above were randomly chosen to fill into the regions defined as the interiors of glassy grains in a nanostructured model, forming HNG models containing glassy grains with different sizes varying from 3 to 32 nm. Secondly, the adjacent glassy grains were prevented from being too close with each other. *i.e.*, the distances among those atoms across surfaces of glassy grains were restricted to be larger than 1 nm, thereby forming HNG models with well separated glassy grains, as illustrated in Figure 1. Subsequently, the HNG models were kept at 300 K for 20 ns in MD simulations to equilibrate the free surfaces of glassy grains in the systems. Thirdly, the HNG model systems were compacted under the hydrostatic pressure of 1 bar, followed by annealing at 500 K and subsequent cooling to 300 K; Consequently, GGIs could be formed among glassy grains in Zr-Cu HNGs. Finally, Zr-Cu HNG models composed of glassy grains with heterogenous compositions interconnected by 30–150 GGIs were obtained. In this work, Zr-Cu HNGs with various average sizes of glassy grains, *i.e.*, $D_{avg} = 3, 5, 7, 10$ and 15 nm, had been constructed for MD simulations and the room-temperature uniaxial tensile tests had been performed on Zr-Cu HNGs at a constant strain rate of 3×10^7 s⁻¹ in the x direction. There were lateral tractions in the y and z directions, and the temperature was kept at 300 K throughout the tensile loading processes, which were controlled by the canonical ensemble and visualized by the OVITO software packages (Stukowski, 2010).

3 Results and discussions

The mechanical properties of Zr-Cu HNGs are determined from the stress versus strain curves obtained by MD simulations,



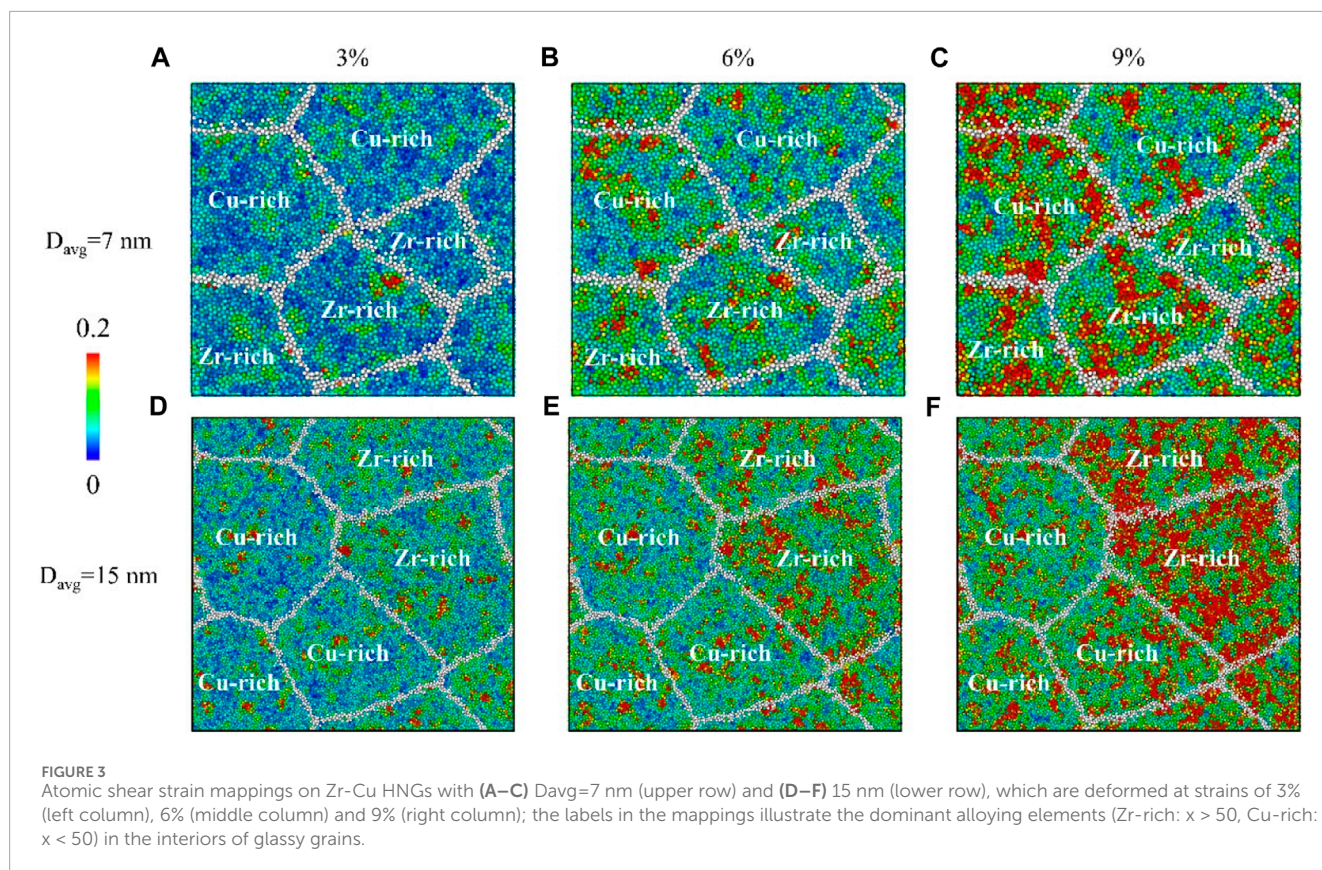
which have been presented in Figure 2A. If D_{avg} is reduced from 15 to 10 nm, the UTS of Zr-Cu HNGs would increase from 2.46 to 3.05 GPa, exhibiting a Hall–Petch like relation. In contrast, the UTS starts gradually decreasing to 2.77 GPa when D_{avg} of Zr-Cu HNGs has been further reduced to 3 nm, resulting in an inverse Hall–Petch like relation illustrated in Figure 2B. Therefore, it is evidential that there exists a critical value of D_{avg} , which is about 10 nm, for the Zr-Cu HNGs studied in this work. With such critical D_{avg} , UTS of Zr-Cu HNGs is the maximum. It is noteworthy that the grain-size effects on the UTS for Zr-Cu HNGs is much different from those for Zr-Cu NGs containing glassy grains with a same chemical composition (Adibi et al., 2014; 2015), which exhibit an inverse Hall–Petch like relation only. It is thus remarkable that the Zr-Cu HNGs would possess mechanical properties with an outstanding combination of the mechanical strength and the tensile ductility

when their D_{avg} is tuned to the critical value, as demonstrated by the tensile curves in Figure 2A. Nonetheless, an experimental study that reports the mechanical properties of HNGs is currently unavailable, which prevent us to further validating the simulation results.

Figure 3 shows the deformation of Zr-Cu HNGs with $D_{avg} = 7$ and 15 nm at atomic scales and shear transformation zone (STZ) or embryonic shear band is recognized as a region under plastic deformation with an atomic shear strain equal to or greater than 0.2, which is defined as follows (Falk and Langer, 1998; Shimizu et al., 2007; Cheng et al., 2009):

$$\eta_i = (J_i J_i^T - I)/2, \quad (1)$$

$$\eta_i^{Mises} = \sqrt{\eta_{ix}^2 + \eta_{iz}^2 + \eta_{iy}^2 + [(\eta_{xx} - \eta_{yy})^2 + (\eta_{xx} - \eta_{zz})^2 + (\eta_{yy} - \eta_{zz})^2]}/6, \quad (2)$$



where η_i is the local Lagrange strain matrix for atom i , J_i is the local transformation matrix for atom i and η_i^{Mises} is the local shear strain for atom i . As it can be seen in Figure 1, Zr-Cu HNGs are heterogeneous in the chemical compositions since the Zr content x for each glassy grain is randomly chosen between $x = 25$ to 75. For simplicity, glassy grains in HNGs are classified into two different categories based on the types of their dominant elements, namely, glassy grains with compositions $x > 50$ and $x < 50$, which are dominated by Zr and Cu atoms, respectively. Clearly, embryonic shear bands start initiating when Zr-Cu HNGs are under plastic deformation at the strain of 3%. After reaching the strain of 9%, both systems would deform heterogeneously with nucleation of STZs either inside the glassy grains or from the GGIs. Nevertheless, for Zr-Cu HNGs with $D_{\text{avg}} = 15$ nm, the number of embryonic shear bands in the interiors of glassy grains with $x > 50$ is prominent, suggesting that the glassy grains with chemical compositions dominated by alloying element Zr have contributed significantly to the mechanical properties of Zr-Cu HNGs (with $D_{\text{avg}} > 10$ nm). In contrast, for Zr-Cu HNGs with $D_{\text{avg}} = 7$ nm, the shear banding in glassy grains with $x > 50$ would not be much different from those in glassy grains with $x < 50$. It is thus suggested that, for Zr-Cu HNG with $D_{\text{avg}} < 10$ nm, the number of STZs in the interiors of glassy grains with Zr content $x > 50$ is similar to that in the glassy grains with dominant Cu atoms ($x < 50$). It is then supposed that the GGIs could alternate the shear banding in Zr-Cu HNGs, and the inverse Hall–Petch like relation determined for UTS is attributed to the GGIs in HNGs with $D_{\text{avg}} < 10$ nm.

Figure 4A shows the histogram plots of chemical compositions of GGIs in Zr-Cu HNGs, demonstrating that GGIs could have a mean chemical composition with a Zr content of $x' = 50$. Figure 4B shows typical concentration profiles across a GGI between two adjacent glassy grains. It is worth noting that these two glassy grains have Zr contents of $x = 63$ and 43, and the GGI composition determined with a Zr content of $x' = 50$ is not simply the average of Zr contents x of those two adjacent glassy grains. Therefore, it is evidential that the atomic structures of GGIs could much differ from those in the interiors of glassy grains. Figure 5 shows the histogram plots for atomic volumes of GGIs in the Zr-Cu HNGs. In general, atomic structures of GGIs are less dense, whose atomic volume (17.7 \AA^3) determined from Figure 5A is larger than that (17.2 \AA^3) for the interiors of glassy grains, meaning that the excess free volumes would be created in the GGI regions. The histogram plots for atomic internal energy of GGIs are shown in Figure 5B, demonstrating that the atomic internal energy ($U = -4.87 \text{ eV/atom}$) of GGIs is higher than that ($U = -4.93 \text{ eV/atom}$) of the glassy grains. In other words, the atomic structures of GGIs containing excess free volumes could be thermodynamically unstable. Figure 5C demonstrates the dependence of atomic volume of glassy grains on the chemical compositions. Obviously, there is an increase in the number of free volumes for glassy grains once if the Zr content x has been increased. Thus, glassy grains with Zr contents $x > 50$ are suggested to be less dense, as compared to those with chemical compositions dominated by alloying element Cu. Furthermore, the composition-dependent internal energy illustrated in Figure 5D clearly manifests the fact

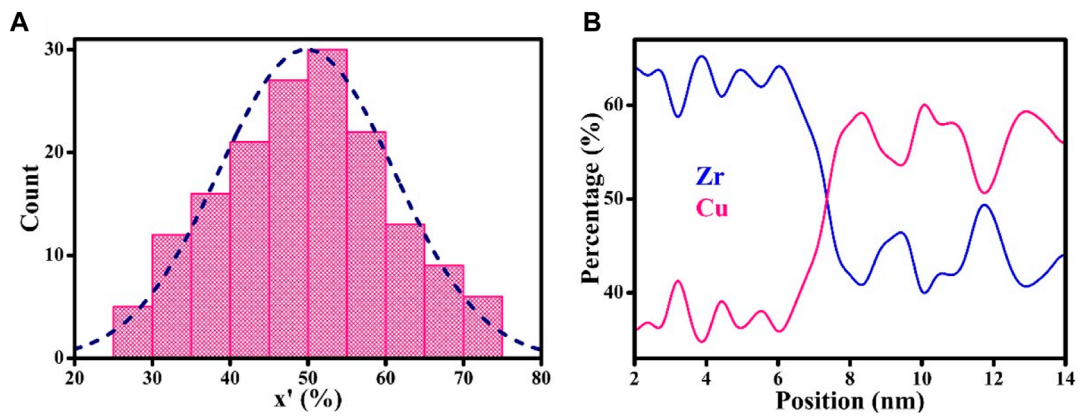


FIGURE 4 (A) The histogram plots on the chemical compositions of GGIs in Zr-Cu HNGs; the dash curve is the fitted profile of the distribution. (B) The elemental concentrations across these two adjacent glassy grains with Zr contents of $x = 63$ and 42 ; the cross point in the concentration profiles suggests that the GGI has a Zr content of $x' = 50$.

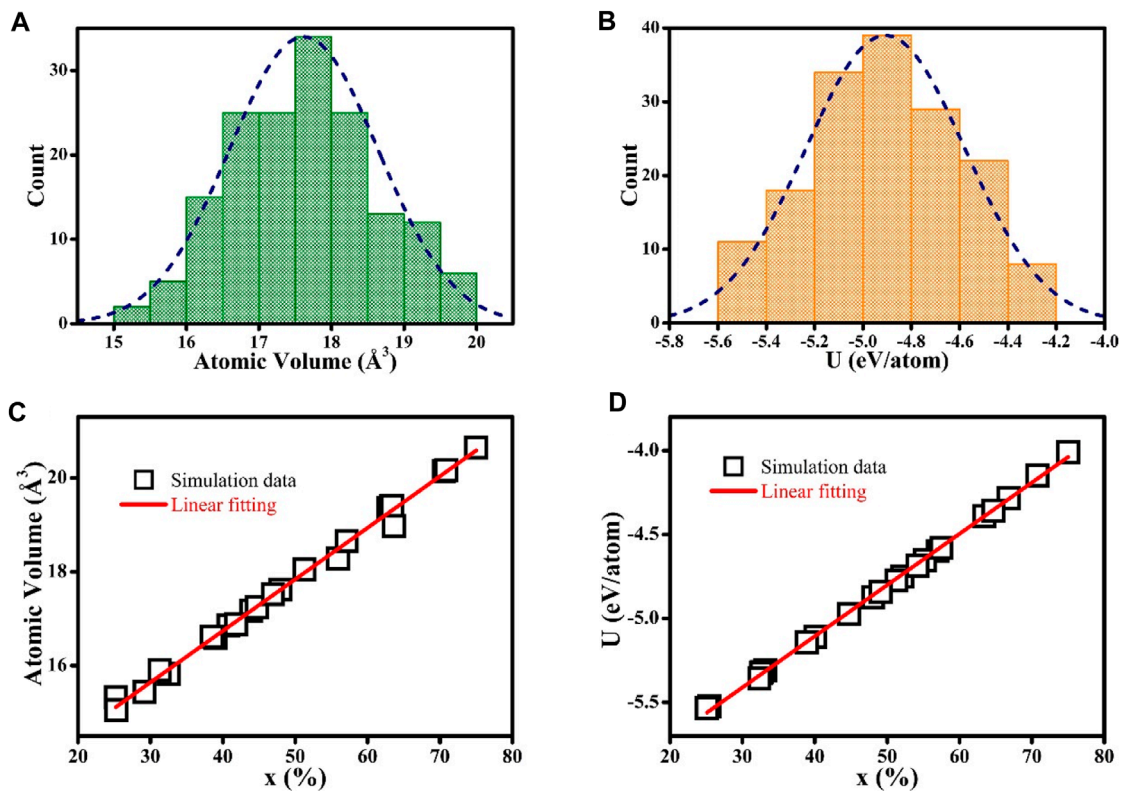


FIGURE 5 The histogram plots on the atomic volume (A) and atomic internal energy U (B) of GGIs in Zr-Cu HNGs; the dash curves are the fitted profiles of the distributions. The atomic volume (C) and atomic internal energy U (D) of glassy grains depend on Zr contents x ($25 \leq x \leq 75$); the lines are the guides to the eye.

that the glassy grains with Zr contents of $x > 50$ are in much higher energy states and, similarly, this outcome is caused by the increasing number of free volumes resulting from an increased Zr content x in the interiors of glassy grains.

Figure 6A presents the grain-size effects on the peak intensities of the radial distribution functions (RDFs) determined for Zr-Cu HNGs. As it can be seen, the intensity of the first RDF peak would decrease when D_{avg} is reduced. Moreover, for the second RDF peak,

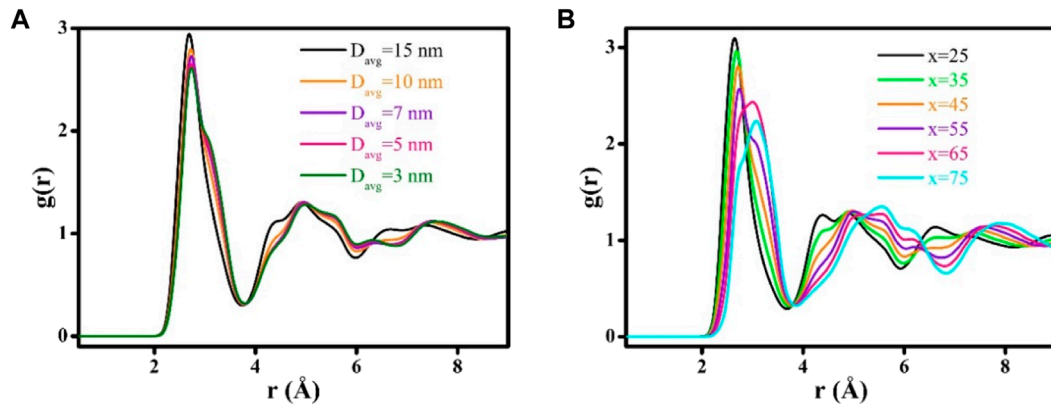


FIGURE 6 The RDF curves of (A) Zr-Cu HNGs with different D_{avg} , and (B) the interiors of glassy grains with various Zr contents x ($25 \leq x \leq 75$).

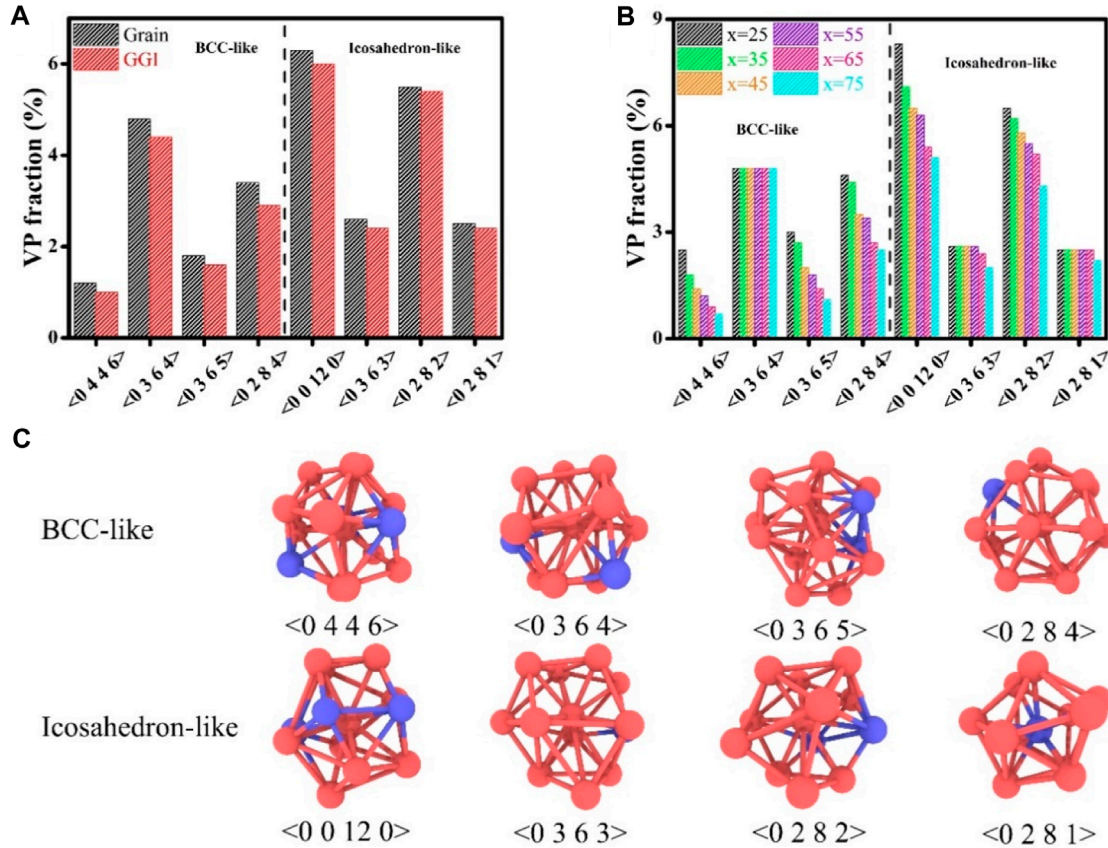


FIGURE 7 The fractions of VPs (A) at GGIs and in the interiors of glassy grains. The VP fractions for glassy grains with various Zr contents x ($25 \leq x \leq 75$) are illustrated in (B). (C) Schematics of bcc- and icosahedron-like VPs.

a decrease and an increase in the intensities have been identified at the radius distances of 4.34 and 5.61 Å, respectively, when D_{avg} of Zr-Cu HNGs is reduced. Considering the increasing volume fraction of GGIs with decreasing D_{avg} , the formation of GGIs is thus suggested to be responsible for the influences of sizes of glassy grains on the intensities of RDF peaks. The RDF curves for glassy

grains with Zr contents $x = 25$ to 75 are separately evaluated and illustrated in Figure 6B. For the first RDF peak, the reduction of intensity with increasing Zr content x is found to be dramatic and, at the same time, its RDF peak position would shift from 2.64 to 3.08 Å as the Zr content increases from $x = 25$ to 75. Furthermore, there are substantial decrease (4.38 Å) and increase (5.55 Å) in

intensities of second RDF peak when the Zr content x is increased, suggesting that the atomic structures of glassy grains resulting from an increased Zr content x have been much altered by alloying element Zr.

The Voronoi polyhedrons (VPs) have been analyzed to probe the topological structures of Zr-Cu HNGs with heterogenous chemical compositions, which are presented in Figures 7A, B. The Voronoi index, $\langle n_3 n_4 n_5 n_6 \rangle$, represents a VP consisting of n_3 , n_4 , n_5 and n_6 numbers of polyhedron faces with 3, 4, 5 and 6 edges, respectively. It is worth noting that the bcc- and icosahedron-like VPs normally possess a coordination number ($n_3+n_4+n_5+n_6$) of 13–14 and 11–12, respectively, which are all dominant in the overall population of VPs, as visualized in Figure 7C. In general, amorphous alloys containing more bcc- and icosahedron-like VPs would have a larger shear resistance and exhibit a better mechanical strength, which are harder to deform by externally applied loads. Figure 7A demonstrates that the fractions of both types of VPs have been reduced in the GGI regions, which are attributed to the excess free volumes in the GGI regions. Therefore, atomic structures of GGIs are suggested to have a mechanical strength lower than that of glassy grains, in consistent with the previous work (Feng et al., 2020; Guan et al., 2022) that the GGIs are mechanically weaker than glassy grains, simply because the GGIs possess short-range order only, whose atomic structures could be similar to those of shear bands. Such atomic structures at interfaces would pose great influences to the mechanical properties of Zr-Cu HNGs. A dramatic reduction in bcc- and icosahedron-like VP fractions resulting from the formation of free volumes is evident for glassy grains when Zr content x increases from $x = 25$ to 75, as illustrated by Figure 7B, indicating that the mechanical strength of glassy grains with Zr contents x larger than 50 could be much lower. For Zr-Cu HNGs with an increasing $D_{\text{avg}} > 10$ nm, the mechanical strength of Zr-Cu HNGs depend more on those of glassy grains with Zr contents $x > 50$ since the plastic deformation primarily localizes inside the glassy grains with chemical compositions dominated by Zr atoms, whose mechanical strength is much lower than that would cause the decrease in UTS with increasing D_{avg} . For Zr-Cu HNGs with $D_{\text{avg}} < 10$ nm, the volume fraction of GGIs is high, which could be further increased by reducing the D_{avg} of Zr-Cu HNGs. Thus, the decrease in UTS with decreasing D_{avg} could result from an increase in the volume fraction of GGIs, whose atomic structures possess a mechanical strength lower than that of glassy grains. In other words, it is the synergy of the increasing volume fraction of GGIs and the existence of glassy grains with Zr contents x larger than 50 that leads to this dependence of UTS on D_{avg} , as determined for Zr-Cu HNGs with heterogenous chemical compositions.

4 Conclusion

In summary, Zr-Cu HNGs composed of glassy grains with different chemical compositions have been studied by MD simulations in this work, and both Hall–Petch like and inverse Hall–Petch like relation are determined for Zr-Cu HNGs. The obtained results show that UTS would decrease with decreasing and increasing D_{avg} of Zr-Cu HNGs when $D_{\text{avg}} < 10$ nm and $D_{\text{avg}} > 10$ nm, respectively. Since GGIs have a mechanical strength lower than that in the interiors of glassy grains, such decrease

in the UTS with decreasing D_{avg} could then be attributed to an increased volume fraction of GGIs. In contrast, the glassy grains with chemical compositions $\text{Zr}_x\text{Cu}_{100-x}$ dominated by Zr (*i.e.*, $x > 50$) are responsible for the decrease in UTS with increasing D_{avg} . Consequently, there exists a maximum of UTS at the critical D_{avg} (~ 10 nm) for the Zr-Cu HNGs with heterogenous compositions. The obtained results demonstrate that the tradeoff issue of strength-ductility for NGs could be resolved by developing HNGs containing glassy grains with different chemical compositions, which is beneficial to facilitating the practical application of NGs.

Data availability statement

The original contributions presented in the study are included in the article/Supplementary Material, further inquiries can be directed to the corresponding authors.

Author contributions

TL: Data curation, Formal Analysis, Funding acquisition, Investigation, Methodology, Software, Validation, Visualization, Writing–original draft, Writing–review and editing. NL: Writing–review and editing. BK: Supervision, Writing–review and editing. GZ: Funding acquisition, Supervision, Writing–review and editing.

Funding

The author(s) declare that financial support was received for the research, authorship, and/or publication of this article. This work was supported by the CDGM Glass Co., Ltd., China, by the Chengdu Guangming Paite Precious Metal Co., Ltd., China, and by the Research Grants Council of Hong Kong Special Administrative Region, China (grant number: 15233823).

Conflict of interest

Authors TL, NL, and BK were employed by CDGM Glass Co., Ltd. Author TL was employed by Chengdu Guangming Paite Precious Metal Co., Ltd.

The remaining author declares that the research was conducted in the absence of any commercial or financial relationships that could be construed as a potential conflict of interest.

The authors declare that this study received funding from the CDGM Glass Co., Ltd. The funder had the following involvement with the study: study design. The authors declare that this study received funding from the Chengdu Guangming Paite Precious Metal Co., Ltd. The funder had the following involvement with the study: the decision to submit it for publication.

Publisher's note

All claims expressed in this article are solely those of the authors and do not necessarily represent those of their affiliated

organizations, or those of the publisher, the editors and the reviewers. Any product that may be evaluated in this article, or claim that may be made by its manufacturer, is not guaranteed or endorsed by the publisher.

References

- Adibi, S., Branicio, P. S., and Joshi, S. P. (2015). Suppression of shear banding and transition to necking and homogeneous flow in nanoglass nanopillars. *Sci. Rep.* 5, 15611. doi:10.1038/srep15611
- Adibi, S., Branicio, P. S., Zhang, Y. W., and Joshi, S. P. (2014). Composition and grain size effects on the structural and mechanical properties of CuZr nanoglasses. *J. Appl. Phys.* 116, 043522. doi:10.1063/1.4891450
- Adjaoud, O., and Albe, K. (2021). Nanoindentation of nanoglasses tested by molecular dynamics simulations: influence of structural relaxation and chemical segregation on the mechanical response. *Front. Mater.* 8, 664220. doi:10.3389/fmats.2021.664220
- Ashby, M. F., and Greer, A. L. (2006). Metallic glasses as structural materials. *Scr. Mater.* 54, 321–326. doi:10.1016/j.scriptamat.2005.09.051
- Averback, R. S., Hahn, H., Höfler, H. J., and Logas, J. C. (1990). Processing and properties of nanophase amorphous metallic alloys: Ni-Ti. *Appl. Phys. Lett.* 57, 1745–1747. doi:10.1063/1.104054
- Baksi, A., Nandam, S. H., Wang, D., Kruk, R., Chellali, M. R., Ivanisenko, J., et al. (2020). Ni₆₀Nb₄₀ nanoglass for tunable magnetism and methanol oxidation. *ACS Appl. Nano Mater.* 3, 7252–7259. doi:10.1021/acsanm.0c01584
- Chen, N., Louzguine-Luzgin, D. V., and Yao, K. (2017). A new class of non-crystalline materials: nanogranular metallic glasses. *J. Alloys Compd.* 707, 371–378. doi:10.1016/j.jallcom.2016.11.304
- Chen, N., Wang, D., Feng, T., Kruk, R., Yao, K. F., Louzguine-Luzgin, D. V., et al. (2015). A nanoglass alloying immiscible Fe and Cu at the nanoscale. *Nanoscale* 7, 6607–6611. doi:10.1039/c5nr01406a
- Cheng, J., Li, T., Ullah, S., Luo, F., Wang, H., Yan, M., et al. (2020). Giant magnetocaloric effect in nanostructured Fe-Co-P amorphous alloys enabled through pulse electrodeposition. *Nanotechnology* 31, 385704. doi:10.1088/1361-6528/ab9971
- Cheng, Y. Q., Cao, A. J., and Ma, E. (2009). Correlation between the elastic modulus and the intrinsic plastic behavior of metallic glasses: the roles of atomic configuration and alloy composition. *Acta Mater.* 57, 3253–3267. doi:10.1016/j.actamat.2009.03.027
- Falk, M. L., and Langer, J. S. (1998). Dynamics of viscoplastic deformation in amorphous solids. *Phys. Rev. E* 57, 7192–7205. doi:10.1103/physreve.57.7192
- Fang, J. X., Vainio, U., Puff, W., Würschum, R., Wang, X. L., Wang, D., et al. (2012). Atomic structure and structural stability of Sc₇₅Fe₂₅ nanoglasses. *Nano Lett.* 12, 458–463. doi:10.1021/nl2038216
- Feng, S. D., Liu, Y. D., Wang, L. M., and Liu, R. P. (2020). Heterogeneous microstructure of Zr₄₆Cu₄₆Al₈ nanoglasses studied by quantifying glass-glass interfaces. *J. Non. Cryst. Solids* 546, 120265.
- Franke, O., Leisen, D., Gleiter, H., and Hahn, H. (2014). Thermal and plastic behavior of nanoglasses. *J. Mater. Res.* 29, 1210–1216. doi:10.1557/jmr.2014.101
- Ghafari, M., Mu, X., Bednarčík, J., Hutchison, W. D., Gleiter, H., and Campbell, S. J. (2020). Magnetic properties of iron clusters in Sc₂₅Fe₇₅ nanoglass. *J. Magn. Magn. Mater.* 494, 165819. doi:10.1016/j.jmmm.2019.165819
- Gleiter, H. (2013). Nanoglasses: a new kind of noncrystalline materials. *Beilstein J. Nanotechnol.* 4, 517–533. doi:10.3762/bjnano.4.61
- Gleiter, H. (2016). Nanoglasses: a new kind of noncrystalline material and the way to an age of new technologies? *Small* 12, 2225–2233. doi:10.1002/smll.201500899
- Gleiter, H., Schimmel, T., and Hahn, H. (2014). Nanostructured solids - from nanoglasses to quantum transistors. *Nano Today* 9, 17–68. doi:10.1016/j.nantod.2014.02.008
- Gu, X. J., Poon, S. J., and Shiflet, G. J. (2007). Mechanical properties of iron-based bulk metallic glasses. *J. Mater. Res.* 22, 344–351. doi:10.1557/jmr.2007.0036
- Guan, Y., Song, W., Wang, Y., Liu, S., and Yu, Y. (2022). Dynamic responses in shocked Cu-Zr nanoglasses with gradient microstructure. *Int. J. Plast.* 149, 103154.
- Guo, C., Fang, Y., Chen, F., and Feng, T. (2019). Nanoindentation creep behavior of electrodeposited Ni-P nanoglass films. *Intermet. (Barking)* 110, 106480. doi:10.1016/j.intermet.2019.106480
- Guo, C., Fang, Y., Wu, B., Lan, S., Peng, G., Wang, X. L., et al. (2017). Ni-P nanoglass prepared by multi-phase pulsed electrodeposition. *Mater. Res. Lett.* 5, 293–299. doi:10.1080/21663831.2016.1264495
- Hirel, P. (2015). Atomsk: a tool for manipulating and converting atomic data files. *Comput. Phys. Commun.* 197, 212–219. doi:10.1016/j.cpc.2015.07.012
- Hu, Q., Wu, J., and Zhang, B. (2017). Synthesis and nanoindentation behaviors of binary CuTi nanoglass films. *Phys. B* 521, 28–31. doi:10.1016/j.physb.2017.06.053
- Inoue, A. (1995). High strength bulk amorphous alloys with low critical cooling rates (overview). *Mater. Trans. JIM* 36, 866–875. doi:10.2320/matertrans1989.36.866
- Inoue, A., Shen, B., Koshiba, H., Kato, H., and Yavari, A. R. (2003). Cobalt-based bulk glassy alloy with ultrahigh strength and soft magnetic properties. *Nat. Mater.* 2, 661–663. doi:10.1038/nmat982
- Jing, J., Krämer, A., Birringer, R., Gleiter, H., and Gonser, U. (1989). Modified atomic structure in a Pd-Fe-Si nanoglass: a Mössbauer study. *J. Non Cryst. Solids* 113, 167–170. doi:10.1016/0022-3093(89)90007-0
- Kalcher, C., Adjaoud, O., and Albe, K. (2020). Creep deformation of a Cu-Zr nanoglass and interface reinforced nanoglass-composite studied by molecular dynamics simulations. *Front. Mater.* 7, 223. doi:10.3389/fmats.2020.00223
- Ketov, S. V., Shi, X., Xie, G., Kumashiro, R., Churyumov, A. Y., Bazlov, A. I., et al. (2015). Nanostructured Zr-Pd metallic glass thin film for biochemical applications. *Sci. Rep.* 5, 7799. doi:10.1038/srep07799
- Klement, W., Willens, R. H., and Duwez, P. (1960). Non-crystalline structure in solidified gold-silicon alloys. *Nature* 187, 869–870. doi:10.1038/187869b0
- Li, F. C., Wang, T. Y., He, Q. F., Sun, B. A., Guo, C. Y., Feng, T., et al. (2018). Micromechanical mechanism of yielding in dual nano-phase metallic glass. *Scr. Mater.* 154, 186–191. doi:10.1016/j.scriptamat.2018.05.050
- Li, T., Ma, K., and Zheng, G. (2021). The effects of glass-glass interfaces on thermodynamic and mechanical properties of Co-Fe-P metallic nano-glasses. *J. Mater. Res.* 36, 4951–4962. doi:10.1557/s43578-021-00429-6
- Li, T., Shen, Y., and Zheng, G. (2021). Characterization on the glass forming ability of metallic nano-glasses by the dynamic scaling for mechanical loss in supercooled liquid state. *Scr. Mater.* 203, 114109. doi:10.1016/j.scriptamat.2021.114109
- Li, T., and Zheng, G. (2021). Atomistic simulation on the mechanical properties of diffusion bonded Zr-Cu metallic glasses with oxidized interfaces. *Metallurgical Mater. Trans. A* 52, 1939–1946. doi:10.1007/s11661-021-06204-w
- Li, T., and Zheng, G. (2022). The anelastic behaviors of Co-Fe-Ni-P metallic nanoglasses: studies on the viscous glass-glass interfaces. *Metallurgical Mater. Trans. A* 53, 3736–3748. doi:10.1007/s11661-022-06781-4
- Li, T., and Zheng, G. (2022). The influences of glass-glass interfaces and Ni additions on magnetic properties of transition-metal phosphide nano-glasses. *AIP Adv.* 12, 085229. doi:10.1063/5.0088043
- Ma, J. L., Song, H. Y., An, M. R., Li, W. W., and Han, R. Q. (2021). A strategy for improving mechanical properties of metallic glass by tailoring interface structure. *J. Non Cryst. Solids* 553, 120464. doi:10.1016/j.jnoncrysol.2020.120464
- Mendelev, M. I., Kramer, M. J., Ott, R. T., Sordelet, D. J., Yagodin, D., and Popel, P. (2009). Development of suitable interatomic potentials for simulation of liquid and amorphous Cu-Zr alloys. *Philos. Mag.* 89, 967–987. doi:10.1080/14786430902832773
- Miroshnichenko, L. S., and Salli, I. V. (1959). Structure of cast iron hardened in liquid state. *Indust. Lab.* 25, 1463–1464.
- Mohri, M., Wang, D., Ivanisenko, J., Gleiter, H., and Hahn, H. (2017). Investigation of the deposition conditions on the microstructure of TiZrCuPd nano-glass thin films. *Mater. Charact.* 131, 140–147. doi:10.1016/j.matchar.2017.07.014
- Mohri, M., Wang, D., Ivanisenko, J., Gleiter, H., and Hahn, H. (2018). Thermal stability of the Ti-Zr-Cu-Pd nano-glass thin films. *J. Alloys Compd.* 735, 2197–2204. doi:10.1016/j.jallcom.2017.11.387
- Nandam, S. H., Adjaoud, O., Schwaiger, R., Ivanisenko, Y., Chellali, M. R., Wang, D., et al. (2020). Influence of topological structure and chemical segregation on the thermal and mechanical properties of Pd-Si nanoglasses. *Acta Mater.* 193, 252–260. doi:10.1016/j.actamat.2020.03.021
- Nandam, S. H., Ivanisenko, Y., Schwaiger, R., Śniadecki, Z., Mu, X., Wang, D., et al. (2017). Cu-Zr nanoglasses: atomic structure, thermal stability and indentation properties. *Acta Mater.* 136, 181–189. doi:10.1016/j.actamat.2017.07.001
- Nandam, S. H., Schwaiger, R., Kobler, A., Kübel, C., Wang, C., Ivanisenko, Y., et al. (2021). Controlling shear band instability by nanoscale heterogeneities in metallic nanoglasses. *J. Mater. Res.* 36, 2903–2914. doi:10.1557/s43578-021-00285-4

- Pei, C., Zhao, R., Fang, Y., Wu, S., Cui, Z., Sun, B., et al. (2020). The structural and dynamic heterogeneities of Ni-P nanoglass characterized by stress-relaxation. *J. Alloys Compd.* 836, 155506. doi:10.1016/j.jallcom.2020.155506
- Plimpton, S. (1997). Fast parallel algorithms for short-range molecular dynamics. *J. Comput. Phys.* 117, 1–19. doi:10.1006/jcph.1995.1039
- Shao, H., Xu, Y., Shi, B., Yu, C., Hahn, H., Gleiter, H., et al. (2013). High density of shear bands and enhanced free volume induced in $Zr_{70}Cu_{30}Ni_{10}$ metallic glass by high-energy ball milling. *J. Alloys Compd.* 548, 77–81. doi:10.1016/j.jallcom.2012.08.132
- Sharma, A., Nandam, S. H., Hahn, H., and Prasad, K. E. (2021). On the differences in shear band characteristics between a binary Pd-Si metallic and nanoglass. *Scr. Mater.* 191, 17–22. doi:10.1016/j.scriptamat.2020.09.009
- Shen, Y., Zheng, X. C., and Zheng, G. P. (2011). Mechanical properties and crystallization behaviors of microstructured Co-Fe-P amorphous alloys. *Metallurgical Mater. Trans. A* 42, 211–218. doi:10.1007/s11661-010-0437-6
- Shimizu, F., Ogata, S., and Li, J. (2007). Theory of shear banding in metallic glasses and molecular dynamics calculations. *Mater. Trans.* 48, 2923–2927. doi:10.2320/matertrans.mj200769
- Singh, S. P., Chellali, M. R., Boll, T., Gleiter, H., and Hahn, H. (2023). Nano-alloying and nano-chemistry of the immiscible elements Fe and Cu in a FeSc-Cu nanoglass. *Mater. Adv.* 4, 2604–2611. doi:10.1039/d3ma00167a
- Sniaidecki, Z., Wang, D., Ivanisenko, Y., Chakravadhanula, V. S. K., Kübel, C., Hahn, H., et al. (2016). Nanoscale morphology of $Ni_{50}Ti_{45}Cu_5$ nanoglass. *Mater. Charact.* 113, 26–33. doi:10.1016/j.matchar.2015.12.025
- Stukowski, A. (2010). Visualization and analysis of atomistic simulation data with OVITO—the Open Visualization Tool. *Model. Simul. Mat. Sci. Eng.* 18, 015012. doi:10.1088/0965-0393/18/1/015012
- Vasantham, S. K., Boltynjuk, E., Nandam, S. H., Berganza Eguarte, E., Fuchs, H., Hahn, H., et al. (2023). Nanoscale confinement of dip-pen nanolithography written phospholipid structures on CuZr nanoglasses. *Adv. Mater. Interfaces* 11, 2300721. doi:10.1002/admi.202300721
- Voigt, H., Rigoni, A., Boltynjuk, E., Chellali, M. R., Tyler, B., Rösner, H., et al. (2023). Evidence for glass–glass interfaces in a columnar Cu–Zr nanoglass. *Adv. Funct. Mater.* 33, 2302386. doi:10.1002/adfm.202302386
- Voigt, H., Rigoni, A., Boltynjuk, E., Rösner, H., Hahn, H., and Wilde, G. (2023). *In situ* TEM studies of relaxation dynamics and crystal nucleation in thin film nanoglasses. *Mater. Res. Lett.* 11, 1022–1030. doi:10.1080/21663831.2023.2278597
- Wang, C., Wang, D., Mu, X., Goel, S., Feng, T., Ivanisenko, Y., et al. (2016). Surface segregation of primary glassy nanoparticles of $Fe_{90}Sc_{10}$ nanoglass. *Mater. Lett.* 181, 248–252. doi:10.1016/j.matlet.2016.05.189
- Wang, J. Q., Chen, N., Liu, P., Wang, Z., Louzguine-Luzgin, D. V., Chen, M. W., et al. (2014). The ultrastable kinetic behavior of an Au-based nanoglass. *Acta Mater.* 79, 30–36. doi:10.1016/j.actamat.2014.07.015
- Wang, X., Jiang, F., Hahn, H., Li, J., Gleiter, H., Sun, J., et al. (2016). Sample size effects on strength and deformation mechanism of $Sc_{75}Fe_{25}$ nanoglass and metallic glass. *Scr. Mater.* 116, 95–99. doi:10.1016/j.scriptamat.2016.01.036
- Wang, X. D., Cao, Q. P., Jiang, J. Z., Franz, H., Schroers, J., Valiev, R. Z., et al. (2011). Atomic-level structural modifications induced by severe plastic shear deformation in bulk metallic glasses. *Scr. Mater.* 64, 81–84. doi:10.1016/j.scriptamat.2010.09.015
- Wang, X. L., Jiang, F., Hahn, H., Li, J., Gleiter, H., Sun, J., et al. (2015). Plasticity of a scandium-based nanoglass. *Scr. Mater.* 98, 40–43. doi:10.1016/j.scriptamat.2014.11.010
- Yang, Q., Pei, C.-Q., Yu, H.-B., and Feng, T. (2021). Metallic nanoglasses with promoted β -relaxation and tensile plasticity. *Nano Lett.* 21, 6051–6056. doi:10.1021/acs.nanolett.1c01283
- Yuan, S., and Branicio, P. S. (2021). Tuning the mechanical properties of nanoglass-metallic glass composites with brick and mortar designs. *Scr. Mater.* 194, 113639. doi:10.1016/j.scriptamat.2020.113639
- Zheng, G. P., Gross, D., and Li, M. (2005). The effect of microstructure on magnetic phase transitions in an Ising model. *Phys. A* 355, 355–373. doi:10.1016/j.physa.2005.03.022